this high-current electron beam generated by an ultrashort laser pulse means that flashes of γ-rays can be generated (*27*), which can be shorter in duration and thus brighter than those generated by electron beams from contemporary linear accelerators. Similarly, in chemistry, radiolysis and fast kinetic reactions induced by high bunch charge electron beams can be investigated with a time resolution better than 100 fs. Also, focusing a second terawatt laser on the electron beam by a pump-probe technique can generate a short and bright x-ray pulse, which is of interest for the study of fast phenomena in biology and crystallography. A final but important consideration is the rapid evolution of the type of "table-top terawatt laser systems" used in this study. Today these cost about 1 million euros and operate at 10 Hz. It is expected that their repetition rate will be increased in the near future to the kHz regime while their cost will be reduced. Consequently, the availability of such laser-plasma accelerators for universities and small laboratories promises to open up a broad spectrum of research in the near future.

References and Notes

1. T. Tajima, J. Dawson, *Phys. Rev. Lett.* **43**, 267 (1979).
2. A. Modena *et al.*, *Nature* **377**, 606 (1995).
3. M. I. Santala *et al.*, *Phys. Rev. Lett.* **86**, 1227 (2001).
4. E. Esarey, P. Sprangle, J. Krall, A. Ting, *IEEE Trans. Plasma Sci.* **24**, 252 (1996), and references therein.
5. E. Esarey, J. Krall, P. Sprangle, *Phys. Rev. Lett.* **72**, 2887 (1994).
6. N. E. Andreev, L. M. Gorbunov, V. I. Kirsanov, A. A. Pogosova, R. R. Ramazashvili, *JETP Lett.* **55**, 571 (1992).
7. T. M. Antonsen, P. Mora, *Phys. Rev. Lett.* **69**, 2204 (1992).
8. P. Sprangle, E. Esarey, J. Krall, G. Joyce, *Phys. Rev. Lett.* **69**, 2200 (1992).
9. C. E. Clayton *et al.*, *Phys. Rev. Lett.* **81**, 100 (1998).
10. A. Ting *et al.*, *Phys. Rev. Lett.* **77**, 5377 (1996).
11. S. P. LeBlanc *et al.*, *Phys. Rev. Lett.* **77**, 5381 (1996).
12. D. Gordon *et al.*, *Phys. Rev. Lett.* **80**, 10 (1998).
13. C. I. Moore *et al.*, *Phys. Rev. Lett.* **79**, 3909 (1997).
14. C. D. Decker, W. B. Mori, K. C. Tzeng, T. Katsouleas, *Phys. Plasmas* **3**, 2047 (1996).
15. W. P. Leemans *et al.*, *IEEE Trans. Plasma Sci.* **24**, 331 (1996).
16. A. Pukhov, J. Meyer-ter-Vehn, *Appl. Phys. B* **74**, 355 (2002).
17. Z. Najmudin *et al.*, *IEEE Trans. Plasma Sci.* **28**, 1057 (2000).
18. A. I. Akhiezer, R. V. Polovin, *Sov. Phys. JETP* **3**, 696 (1956).
19. S. V. Bulanov, V. I. Kirsanov, A. S. Sakharov, *Sov. Phys. JETP* **50**, 198 (1989).
20. A. Pukhov, Z.-M. Zheng, J. Meyer-ter-Vehn, *Phys. Plasmas* **6**, 2847 (1998).
21. M. Pittman *et al.*, *Appl. Phys. B* **74**, 529 (2002).
22. D. Strickland, G. Mourou, *Opt. Commun.* **56**, 219 (1985).
23. C. D. Decker, D. C. Eder, R. A. London, *Phys. Plasmas* **3**, 414 (1996).
24. V. Malka *et al.*, *Rev. Sci. Instrum.* **71**, 2329 (2000).
25. Y. Yamazaki, T. Kurihara, H. Kobayashi, I. Sato, A. Asami, *Nucl. Instrum. Methods A* **322**, 139 (1992).
26. S. Fritzler *et al.*, in preparation.
27. R. D. Edwards *et al.*, *Appl. Phys. Lett.* **80**, 2129 (2002).

28. This work was partially supported by the EU Access to Research Infrastructure under LOA Contract HPRI-1999-CT-00086.

30 July 2002; accepted 15 October 2002

Fluorometric Detection of Enzyme Activity with Synthetic Supramolecular Pores

Gopal Das, Pinaki Talukdar, Stefan Matile*

The reversible blockage of synthetic pores formed by rigid-rod β barrels, either by substrates or products, was used to sense a variety of enzymatic reactions in high-throughput format with "naked-eye" fluorescent detection. Improvement of sensor sensitivity beyond three orders of magnitude by straightforward internal mutations underscores the functional plasticity of rigid-rod β barrels. Such detectors of enzyme activity with the aforementioned characteristics are needed in areas as diverse as proteomics and environmentally benign organic synthesis.

A promising approach for analyzing biological molecules is to harness the selectivity of transmembrane pores. Such approaches usually require the engineering of natural (*1, 2*) or artificial (*3–9*) pores, so that they are selectively blocked by an analyte of interest, and a detection scheme, often the determination of ion currents.

Rather than rely on the complexities of measuring ion currents to detect an analyte of interest, we devised a fluorescent dye method to determine the progress of enzymatic reactions that convert good pore blockers into poor ones (or poor blockers into good ones). Methods that allow enzymatic activity to be screened rapidly are needed both for developing new reaction routes, such as in carbohydrate synthesis (*10–12*), and for identifying enzyme inhibitors for pharmaceutical use (*13, 14*). Many enzymes of interest are phosphatases that convert a substrate, such as adenosine triphosphate (ATP), into smaller molecules, such as adenosine monophosphate (AMP) or inorganic phosphate (P_i) (*13, 15*).

We designed several pores that are blocked to a much larger extent by these larger substrates [as reflected in their dissociation constant (K_D)] than by the smaller reaction products. These pores were introduced into large unilamellar vesicles (LUVs) containing a fluorescent dye at concentrations high enough that emission is self-quenched. The extent of conversion of the substrate of interest (i.e., ATP) will cause differential rates of leakage of the dye from the vesicles, which will be reflected in an increase in fluorescence from the vesicles as self-quenching is diminished.

We used engineered rigid-rod β barrels as the pores. We have previously demonstrated the self-assembly of these synthetic barrel-stave supramolecules (*6–9*). The key element

Department of Organic Chemistry, University of Geneva, CH-1211 Geneva, Switzerland.

*To whom correspondence should be addressed. E-mail: stefan.matile@chiorg.unige.ch

Table 1. Binding of substrates and products to synthetic supramolecular pores. Abbreviations and materials can be found in Fig. 2 and (*18*). Dissociation constants (K_D) are given in micromolar concentration (*17*). ND, not determined.

Entry	Enzyme	Pore	Substrates	K_D (μM)	Products	K_D (μM)
1	Apyrase	**1** ⊃ $Mg^{2+}{}_n$	ATP	6,700*	AMP†	20,400*
2	Apyrase	**2**	ATP	2	AMP†	66
3	Apyrase	**1** ⊃ $Mg^{2+}{}_n$	TPP	10,000*	Thiamine†	>240,000*
4	Apyrase	**2**	TPP	440	Thiamine†	ND
5	Aldolase‡	**1** ⊃ $Mg^{2+}{}_n$	FDP	21,800*	DHAP‡	>150,000
6	Aldolase‡	**2**	FDP	220	DHAP‡	>2,500
7	Alkaline phosphatase	**2**	UDP	1,175	U†	>75,000
8	Galactosyltransferase	**2**	UDPGal	>75,000	UDP	1,175
			GlcNAc	>50,000	Galβ1→GlcNAc	>50,000

*Data from (*8*). †P_i [$H_nPO_4^{-(3-n)}$]: K_D (**1** ⊃ $Mg^{2+}{}_n$) = 66.6 mM (*8*), K_D (**2**) = 12.0 mM. ‡Glyceraldehyde 3-phosphate was converted to dihydroxyacetone phosphate (DHAP) by TIM.

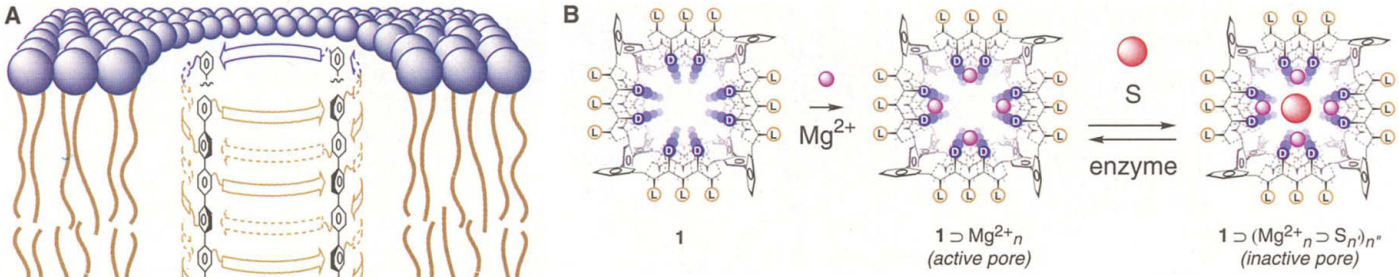

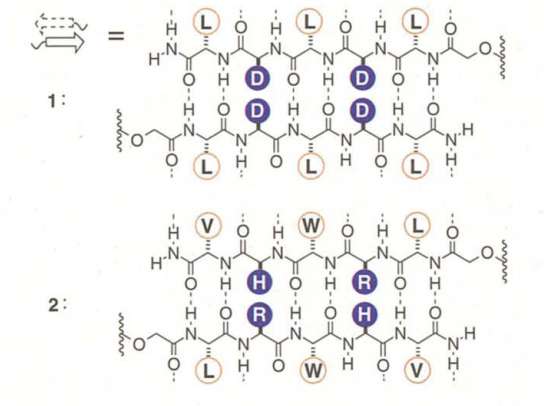

Fig. 1. (**A**) Rigid-rod β barrels **1** and **2** in lipid bilayers, depicted in blue (hydrophilic), gold (hydrophobic), and black (rigid-rod and β-sheet scaffolds); α–amino acid residues located at the outer surface are black on white; internal ones are white on blue (single-letter abbreviations: D, Asp; H, His; L, Leu; R, Arg; V, Val; W, Trp). (**B**) Pore **1** as enzyme detector. Changes in the obstruction of dye efflux from liposomes through host **1** ⊃ $Mg^{2+}{}_n$ by either substrate (S, red) or product (*20*) due to substrate conversion are reported by changes in dye fluorescence; analogous mechanisms are suggested for product blockage and **2** (*17*, *20*).

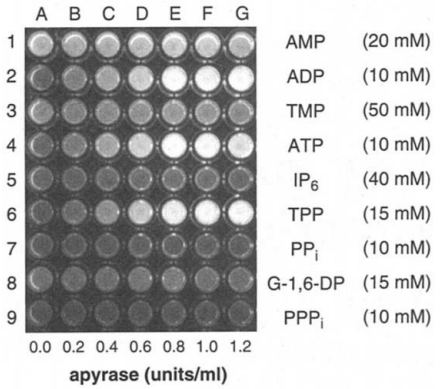

Fig. 2. End-point substrate screening using **1** ⊃ $Mg^{2+}{}_n$. Substrate candidates at $c > K_D$ (lanes 1 to 9) were incubated for 20 hours with increasing apyrase concentrations (lanes A to G). The LUVs ⊃ CF and **1** were then added, and fluorescence was measured within ≤30 min. Increasing CF emission with increasing enzyme concentration correctly identified ADP, ATP, and TPP (lanes 2, 4, 6, respectively) as substrates (*15*, *18*).

is a "stave" created by a *p*-octiphenyl group, to which are attached short peptides containing (2*i* + 1) amino acids. These peptide chains interdigitate with chains from another stave to form a β sheet. Rather than forming an extended plane, the torsion modes of the phenyl groups in the rigid-rod stave appear to force a nonplanar arrangement and lead to the formation of a β barrel. Cylindrical self-assembly with preferential peripheral crowding (*16*) then places amino acid residues *i*, *i* + 2, . . . , at the outer and residues *i* + 1, *i* + 3, . . . , at the inner barrel surface (*6*–*9*).

The design of synthetic multifunctional pores allows us to exploit a simple relation between primary and tertiary structure. In barrel **1**, for instance, external leucines were chosen for hydrophobic contacts with the liquid-crystalline bilayer core, whereas internal aspartates were installed to mediate chemical processes within the pore. As a result, it was possible to "fill" pore **1** in a stepwise manner (Fig. 1B), first with Mg^{2+} and then with a broad variety of anionic substrates. These processes could be easily detected as activation and deactivation of anion permeable pores (*8*). The wide variety of K_D values observed for the latter process suggested that, in the present context, enzyme sensing is possible if one substrate blocks **1** ⊃ $Mg^{2+}{}_n$ (Fig. 1B) with a $K_D{}^{min}$ that is less than half of those of all products, or if the $K_D{}^{min}$ of one product is less than half of those of all substrates (*17*).

Potato apyrase, a nonspecific adenosine triphosphatase (ATPase) that converts ATP into the poor pore blockers P_i and AMP (Table 1), fulfilled this condition (*15*). Therefore, ATP was incubated with increasing concentrations of apyrase for 20 hours at room temperature. To the resulting reaction mixture, LUVs composed of egg yolk phosphatidylcholine (EYPC) and loaded with 5(6)-carboxyfluorescein (CF) at self-quenching concentrations (i.e., EYPC-LUVs ⊃ CF) and **1** were added to the Mg^{2+}-containing reaction mixtures (*18*). Increasing CF emission seen with increasing apyrase concentrations indicated consumption of the blocker by the enzyme. This result confirmed that ATP conversion is indeed readily detectable with metallopore **1** ⊃ $Mg^{2+}{}_n$.

Implementation of noninvasive, high-throughput substrate screening with the possibility of "naked-eye" detection was therefore straightforward (Fig. 2). Nine candidates with known K_D values (*8*, *17*) were placed at concentrations $c > K_D{}^{min}$ in a multiwell plate and incubated with apyrase (*18*). Increasing emission with increasing apyrase concentration after addition of LUVs ⊃ CF and **1** ⊃ $Mg^{2+}{}_n$ identified—consistent with previous studies (*15*)—ATP, adenosine diphosphate (ADP), and thiamine pyrophosphate (TPP) (lanes 2, 4, and 6), but neither AMP, thiamine monophosphate (TMP), phytate (IP_6), pyrophosphate (PP_i), glucose 1,6-diphosphate (G-1,6-DP), nor triphosphate (PPP_i) (lanes 1, 3, 5, and 7 to 9), as substrates.

The screening requirement $c > K_D{}^{min}$ limited sensor sensitivity to 1.3 μmol ATP. Because weak $Mg^{2+}{}_n$ binding was known to account for the high K_D values with pore **1** (*8*), the internal aspartates were replaced by internal arginine-histidine dyads in cationic

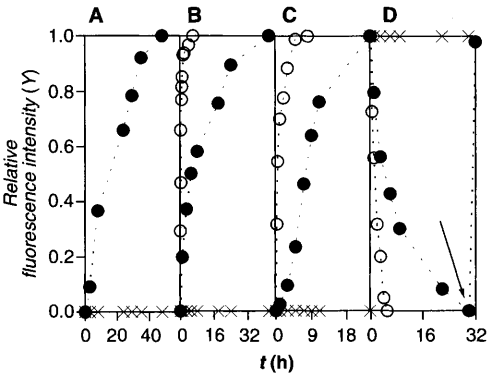

Fig. 3. Real-time enzyme screening with (**A**) apyrase, (**B**) aldolase, (**C**) alkaline phosphatase, and (**D**) galactosyltransferase without and (arrow) with CIAP, using **2**. Fractional pore activity *Y* (*18*) after addition of 20 μl of reaction mixture and **2** to LUVs ⊃ CF is shown as a function of reaction time. Reaction mixtures: (A) 0 (×) and 4 (●) U/ml apyrase, 40 mM ATP; (B) 0 (×), 2 (●), and 16 (○) U/ml RAMA, 750 U/ml triosephosphate isomerase (TIM), 40 mM D-fructose 1,6-diphosphate (FDP); (C) 0 (×), 66 (●), and 670 (○) U/ml CIAP, 800 mM UDP; (D) 0 (×), 8 (●, arrow: addition of 66 U/ml CIAP), and 32 (○) U/ml galactosyltransferase, 250 mM *N*-acetylglucosamine (GlcNAc), 375 mM UDPGal [or 375 mM NAcUDPGal (*20*)] (*18*).

pore **2** (Fig. 1) (*18*). As expected from specific guanidinium-phosphate interactions (*19*), K_D^{min} = 2 μM determined for ATP demonstrated increased sensitivity (by a factor of >1000) of apyrase sensor **2** compared to **1** ⊃ $Mg^{2+}{}_n$ (*17, 18*).

The most important adaptability of pore **2** to sense various enzymes was exemplified with real-time detection of selected classes of enzymes for which noninvasive assays compatible with high-throughput substrate screening for the development of enzymatic carbohydrate and oligosaccharide synthesis (*10–12*) are needed. As with apyrase, rabbit muscle aldolase (RAMA) (*10*) and calf intestine alkaline phosphatase (CIAP) (*11*) converted strong channel blockers into poor ones (Table 1, entries 5 to 7). Enzyme-catalyzed substrate consumption was thus reported by the decreasing ability of the reaction mixture to hinder CF efflux through **2** with increasing reaction time, i.e., "enzymegated" pore formation (Fig. 3, A to C). Bovine milk galactosyltransferase (*11, 12*), in contrast, produced uridine diphosphate (UDP) with K_D^{min} = 1.2 mM from two poor blockers (Table 1, entry 8). This enzyme was therefore detectable by decreasing activity of pore **2** with increasing reaction time (Fig. 3D). Use of CIAP to eliminate UDP blockage (Fig. 3D, arrow) corroborated the proposed mechanism and demonstrated the possibility to detect two enzymes simultaneously or, from a different point of view, to turn synthetic multifunctional pores "off" and "on" using enzymes only.

Taken together, these results demonstrate practical usefulness of synthetic supramolecular pores for fluorometric detection of enzyme activity, a topic of current scientific interest (*13*). The most important characteristic of our assay is adaptability of the same supramolecular sensor to a broad variety of substrates and enzymes. There is no need to prepare new, substrate- or product-specific antibodies [as for catalytic assays using enzyme-linked immunosorbent assay (cat-ELISA) and related assays] or synthetic receptors for individual enzymes; no need to label substrates as in fluorogenic and radioassays; and no need to calibrate coupled multienzyme assays (*13, 14*). Whereas intrinsic limitations concerning, e.g., hydrophobic or lytic substrates, certain more complex analytes (*18*), continuous assay, or in vivo detection will be challenging to overcome, at least in a general manner, there is much room to implement various in vitro formats compatible with high-throughput screening and miniaturization (*1*).

References and Notes

1. H. Bayley, P. S. Cremer, *Nature* **413**, 226 (2001).
2. S. Cheley, L. Gu, H. Bayley, *Chem. Biol.* **9**, 829 (2002).
3. P. Scrimin, P. Tecilla, *Curr. Opin. Chem. Biol.* **3**, 730 (1999).
4. G. W. Gokel, A. Mukhopadhyay, *Chem. Soc. Rev.* **30**, 274 (2001).
5. G. J. Kirkovits, C. D. Hall, *Adv. Supramol. Chem.* **7**, 1 (2000).
6. S. Matile, *Chem. Soc. Rev.* **30**, 158 (2001).
7. G. Das, S. Matile, *Proc. Natl. Acad. Sci. U.S.A.* **99**, 5183 (2002).
8. G. Das, H. Onouchi, E. Yashima, N. Sakai, S. Matile, *Chembiochem* **3**, 1089 (2002).
9. Without high-resolution crystallographic evidence, it is not incorrect to perceive the depicted suprastructures as, at worst, productive working hypotheses that are consistent with all (*6–8*) functions discovered so far.
10. T. D. Machajewski, C.-H. Wong, *Angew. Chem. Int. Ed.* **39**, 1352 (2000).
11. M. M. Palcic, *Methods Enzymol.* **230**, 300 (1994).
12. N. Wymer, E. J. Toone, *Curr. Opin. Chem. Biol.* **4**, 110 (2000).
13. D. Wahler, J.-L. Reymond, *Curr. Opin. Chem. Biol.* **5**, 152 (2001).
14. A. W. Czarnik, *Acc. Chem. Res.* **27**, 302 (1994).
15. M. Komoszynski, A. Wojtczak, *Biochim. Biophys. Acta* **1310**, 233 (1996).
16. G. M. Whitesides *et al.*, *Acc. Chem. Res.* **28**, 37 (1995).
17. All reported K_D values are conditional to the method (Hill analysis of concentration dependence) specified in (*8*).
18. See supporting data on *Science* Online.
19. T. S. Snowden, E. V. Anslyn, *Curr. Opin. Chem. Biol.* **3**, 740 (1999).
20. G. Das, P. Talukdar, S. Matile, data not shown.

21. We thank J.-L. Reymond and N. Sakai for advice, J. Gruenberg for access to still video camera and fluorescence counter, and the Swiss NSF (2000-064818.01 and National Research Program "Supramolecular Functional Materials" 4047-057496) for financial support.

Supporting Online Material

www.sciencemag.org/cgi/content/full/298/5598/1600/DC1
Materials and Methods
References and Notes

14 August 2002; accepted 14 October 2002

Arsenic Mobility and Groundwater Extraction in Bangladesh

Charles F. Harvey,[1] Christopher H. Swartz,[1]* A. B. M. Badruzzaman,[2] Nicole Keon-Blute,[1] Winston Yu,[1] M. Ashraf Ali,[2] Jenny Jay,[1] Roger Beckie,[3] Volker Niedan,[1] Daniel Brabander,[1]† Peter M. Oates,[1] Khandaker N. Ashfaque,[1] Shafiqul Islam,[4] Harold F. Hemond,[1] M. Feroze Ahmed[2]

High levels of arsenic in well water are causing widespread poisoning in Bangladesh. In a typical aquifer in southern Bangladesh, chemical data imply that arsenic mobilization is associated with recent inflow of carbon. High concentrations of radiocarbon-young methane indicate that young carbon has driven recent biogeochemical processes, and irrigation pumping is sufficient to have drawn water to the depth where dissolved arsenic is at a maximum. The results of field injection of molasses, nitrate, and low-arsenic water show that organic carbon or its degradation products may quickly mobilize arsenic, oxidants may lower arsenic concentrations, and sorption of arsenic is limited by saturation of aquifer materials.

In an effort to prevent waterborne disease, Bangladesh shifted its drinking water supply from surface to groundwater. Many of the recently installed 6 to 10 million drinking-water wells contain high concentrations of arsenic (*1*), causing widespread arsenicosis